Journal of Physics: Conference Series

PAPER • **OPEN ACCESS**

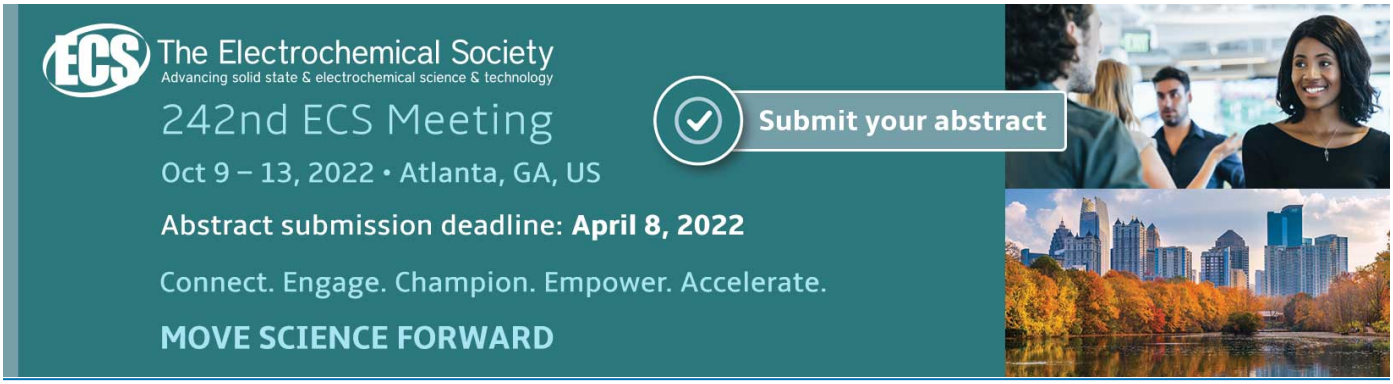
Measurement of Decay Time Constant of Shielding Current in ITER-TF Joint Samples

To cite this article: S Imagawa *et al* 2021 *J. Phys.: Conf. Ser.* **1857** 012013

View the article online for updates and enhancements.

You may also like

- Bulk superconducting tube subjected to the stray magnetic field of a solenoid
K Hogan, J-F Fagnard, L Wéra et al.
- Metastable inhomogeneous vortex configuration with non-uniform filling fraction inside a blind hole array patterned in a BSCCO single crystal and concentrating magnetic flux inside it
Gorky Shaw, S S Banerjee, T Tamegai et al.
- Total loss measurement and simulation in a REBCO coated conductor carrying DC current in perpendicular AC magnetic field at various temperatures
Yueming Sun, Jin Fang, Gennady Sidorov et al.



This content was downloaded from IP address 133.75.110.209 on 01/04/2022 at 06:06

Journal of Physics: Conference Series **1857** (2021) 012013 doi:10.1088/1742-6596/1857/1/012013

Measurement of Decay Time Constant of Shielding Current in ITER-TF Joint Samples

S Imagawa[1], H Kajitani[2], T Obana[1], S Takada[1], S Hamaguchi[1], H Chikaraishi[1], Y Onodera[1], K Takahata[1], K Matsui[2], and N Koizumi[2]

[1] National Institute for Fusion Science, National Institutes of Natural Sciences,
[2] Fusion Energy Research and Development Directorate, National Institute for Quantum and Radiological Science and Technology

imagawa@nifs.ac.jp

Abstract. Joint sample tests have been carried out as a qualification test for ITER Toroidal Field (TF) coils. The joint sample comprises two short TF conductors that have "twin-box" joint terminals at both ends. The lower joint is a testing part that is a full size joint of the TF coils. Hall probes are attached on the lower joint box at around the center of the external field coil of the test facility. The magnetic field induced by shielding currents in the joint can be estimated from the difference between the measured magnetic field strength and the magnetic field generated by the external field coil. The magnetic field by the shielding currents during shut-off of the external field coil from -1.0 T is evaluated for six samples. The decay time constants of the shielding currents are gradually elongated with decrease of the shielding currents in all the samples. In comparison with simulation results, it is considered that the main shielding current flows in superconducting cables in the two conductors with crossing the jointed plane and that the joint resistance is decreased at low total current.

1. Introduction

A Toroidal Field (TF) coil of ITER comprises seven double-pancakes that are connected to each other with "twin-box" joints [1, 2]. The twin-box joint is also adopted for the TF coil terminal. Low electrical resistance in nΩ is attained by direct contact of Nb_3Sn superconducting strands to a copper sleeve of the box and by soldering of adjacent copper sleeve of the two boxes [3, 4]. The required joint resistance of the ITER-TF coil joints is less than 3 nΩ at 2 T of background field. As a qualification test of the ITER-TF coils, their joint samples have been tested prior to manufacture of each TF coil with a conductor test facility, which is equipped with 9 T split coils and a dc 75 kA power supply [5].

The joint sample comprises two short TF conductors that have twin-box joint terminals at both ends. The lower joint is a testing part that is a full size joint of the TF coil. Hall probes are attached on the lower joint box to clarify amount and decay time constant of shielding currents. The magnetic field induced by shielding currents in the joints can be estimated from the difference between the measured magnetic field strength and the magnetic field generated by the external field coil (9 T split coils). In this paper, we intend to summarize the experimental results during shut-off of the external field coil and to discuss the features of the shielding currents as well as the dependence of the joint resistance on the current in comparison with simulation results.

Content from this work may be used under the terms of the Creative Commons Attribution 3.0 licence. Any further distribution of this work must maintain attribution to the author(s) and the title of the work, journal citation and DOI.
Published under licence by IOP Publishing Ltd

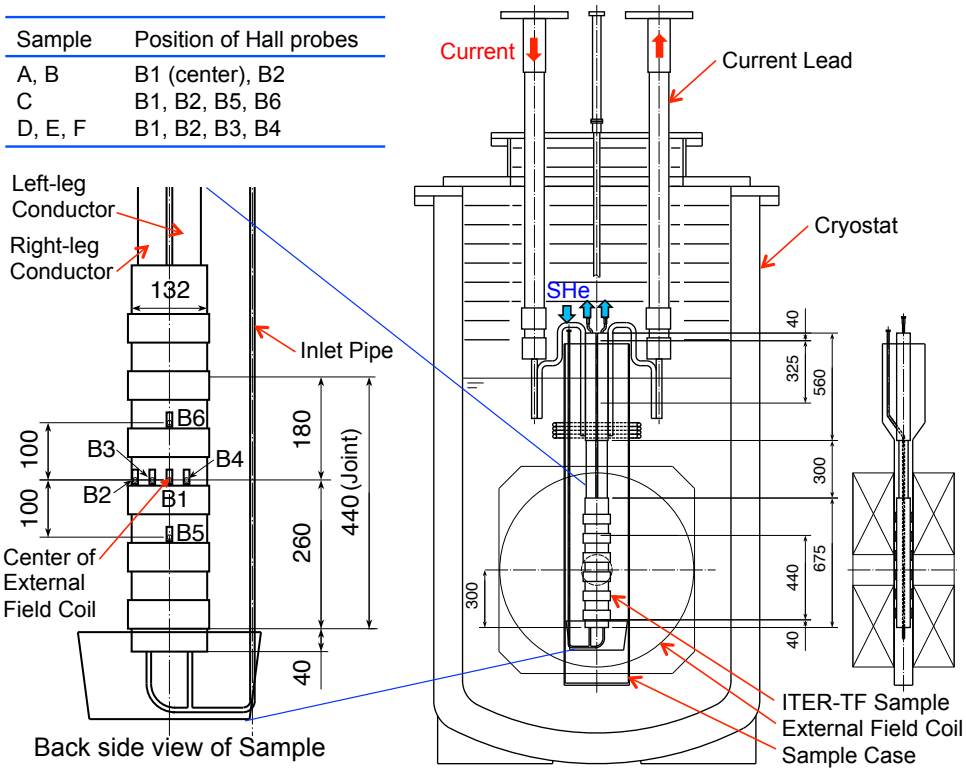


Figure 1. A setup of an ITER-TF joint sample in the 9 T test facility. B1 to B6 show the positions of Hall probes.

2. Experimental set up

An ITER-TF conductor consists of a multi-stage twisted cable, a center channel, and a conduit [4]. The total numbers of Nb_3Sn and copper strands are 900 and 522, respectively. The twist pitches of the cable are 81, 140, 186, 298 and 420 mm for 1st to 5th stage. A joint sample consists of two short TF conductors with 1,535 mm of length, which is restricted by the test facility, as shown in Fig. 1. The lower joint is a testing part that is a full size joint of the TF coil, where the strands contact to the copper sleeve by the length of 440 mm. The total length of the lower joint box is 675 mm including the transition region of cable compaction. The length of the upper joint box is shortened to 560 mm in order to attain the original conductor part of 300 mm length for setting voltage taps. At the joint region, a cable wrap and sub-cable wraps at the outer surface of the cable are removed, and the chromium layer of the cable surface is also removed [4]. The cable is compacted from the void fraction of 33% to 25%. Low contact resistance between the cable and the copper sleeve is achieved by sintering through heat treatment of the sample for production of A15 phase of Nb_3Sn. The copper sleeves of the lower joint are connected to one another using PbSn solder. The upper terminals of the joint sample are attached to copper bus-bars that are attached to the current leads, and the entire assembly is installed into the test facility. The lower joint is set near the center of the external field coil.

Hall probes are attached on the lower joint box at the jointed plane of the two conductors (B1), at the edge of one conductor (B2), and at the middle of one conductor (B3 and B4), as shown in Fig. 1. The vertical (longitudinal) positions of these four Hall probes are the same as the center of the external field coil. B5 and B6 probes are attached for only Sample C at the height of -100 mm and +100 mm, respectively, at the jointed plane. All of the Hall probes measure the field parallel to the axis of the external field coil.

While the external field coil of the test facility is cooled with liquid helium, the joint sample is cooled with supercritical helium (SHe). Therefore, a sample case made from stainless steel is inserted between the 9 T split coils, and the samples are tested in gaseous helium atmosphere. SHe is supplied

from the bottom of the two conductors and exhausted from their top. The temperature of the supplied SHe is controlled from 4.4 K to 6 K with film heaters on the inlet cooling pipe.

3. Experimental results

3.1. Method to estimate shielding currents

Shielding currents induced in the samples can be estimated from the difference between the measured magnetic field strength and the magnetic field generated by the external field coil. Assuming that shielding current just before shut-off is zero, the magnetic field $\Delta B_i(t)$, which is induced by shielding currents at the position of the Hall probe of Bi (i=1, 6), is given by

$$\Delta B_i(t) = B_i(t) - B_i(0)/I_0(0)\cdot I_0(t) \quad (1)$$

where t, $B_i(t)$, and $I_0(t)$ are the time after shut-off, the magnetic field measured with the Hall probe of Bi and the current of the external field coil. An example of $B_1(t)$ and $B_2(t)$ during a shut-off from -1.0 T with an external dump resister is shown in Fig. 2a. Each off-set of zero is estimated from the exponential function that is regressed from the data at the time when the shielding currents are decayed sufficiently. The estimated magnetic fields induced by shielding currents are shown in Fig. 2b.

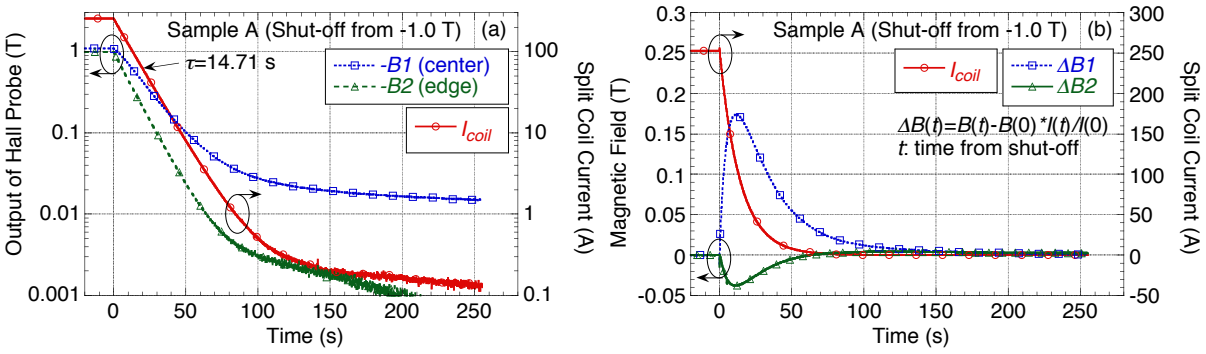


Figure 2. Outputs of Hall probes of B1 and B2 (a) and estimated magnetic fields of ΔB_1 and ΔB_2 induced by shielding currents (b) during shut-off from -1.0 T in Sample A.

3.2. Experimental results

Estimated magnetic fields induced by shielding currents, ΔB_i, are shown in Figs. 3a to 3f with a logarithmic scale for six joint samples of ITER-TF coils. Fig. 3a is the same data as Fig. 2b. Decay time constants of most of ΔB_i are gradually elongated with decrease of the shielding currents. The magnetic field by the shielding currents at the jointed plane, ΔB_1, is higher than that at the middle of one conductor, ΔB_3 or ΔB_4, as shown in Figs. 3d, 3e and 3f. Here we consider three current loops with long decay time constant. One is the largest current loop, Loop 1, where the shielding current flows in two conductors with crossing the jointed plane (see Fig. 5). The other ones are coupling currents in left-leg and right-leg conductors, which are named Loop 2 and Loop 3, respectively. $B_1(t)$, $B_3(t)$ and $B_4(t)$ are affected mainly by Loop 1, by Loop 1 and Loop 2, and by Loop 1 and Loop 3, respectively. In the case of Sample F, the decay time constant of Loop 1 is considered to be shorter than that of Loop 3 because the decrease of ΔB_1 is faster than ΔB_4 after around 80 s from the shut-off, and because ΔB_1 is decreased to the same value as ΔB_4 at 300 s. In the other cases (Samples D and E), the decay time constant of ΔB_1 is longer or equal than ΔB_3 and ΔB_4.

The decay time constants at the beginning of decay are listed in Table 1 with each joint resistance R_j of the joint samples at 4.4 K without external magnetic field. Since the current of Loop 1 crosses the half length of jointed plane twice, the decay time constant of Loop 1 is given by $L/(4R_j)$, where L is the inductance of Loop 1. In other words, the effective inductance of Loop 1 is given by $4R_j\cdot\tau$ where τ is the decay time constant. In the case that τ is longer than 50 s, L is estimated around 0.16 μH that

corresponds to the inductance of a set of parallel conductors with the length of 0.30 m, diameter of 32 mm and distance of 48 mm. In the case of shorter τ, the decay time constant of the external field of 14.7 s can not be ignored. The actual τ can be estimated from the calculation of an electric circuit with a resistor, an inductance (coil), and a voltage source with the decay time constant of 14.7 s, as shown in Fig. 4 in the case of Sample A. The estimated actual τ is shown in brackets in Table 1.

The highest current of Loop 1 depends mainly on R_j, and the value estimated from ΔB_1 and ΔB_3 is in the range of 50 kA. The current of Loop 2 is estimated to be approximately one-half of the current of Loop 1. Therefore, the decrease of the decay time constant of the shielding currents is considered to be caused by the decrease of the joint resistance at low total current, which is discussed in the next section by comparing the experimental data with simulation results.

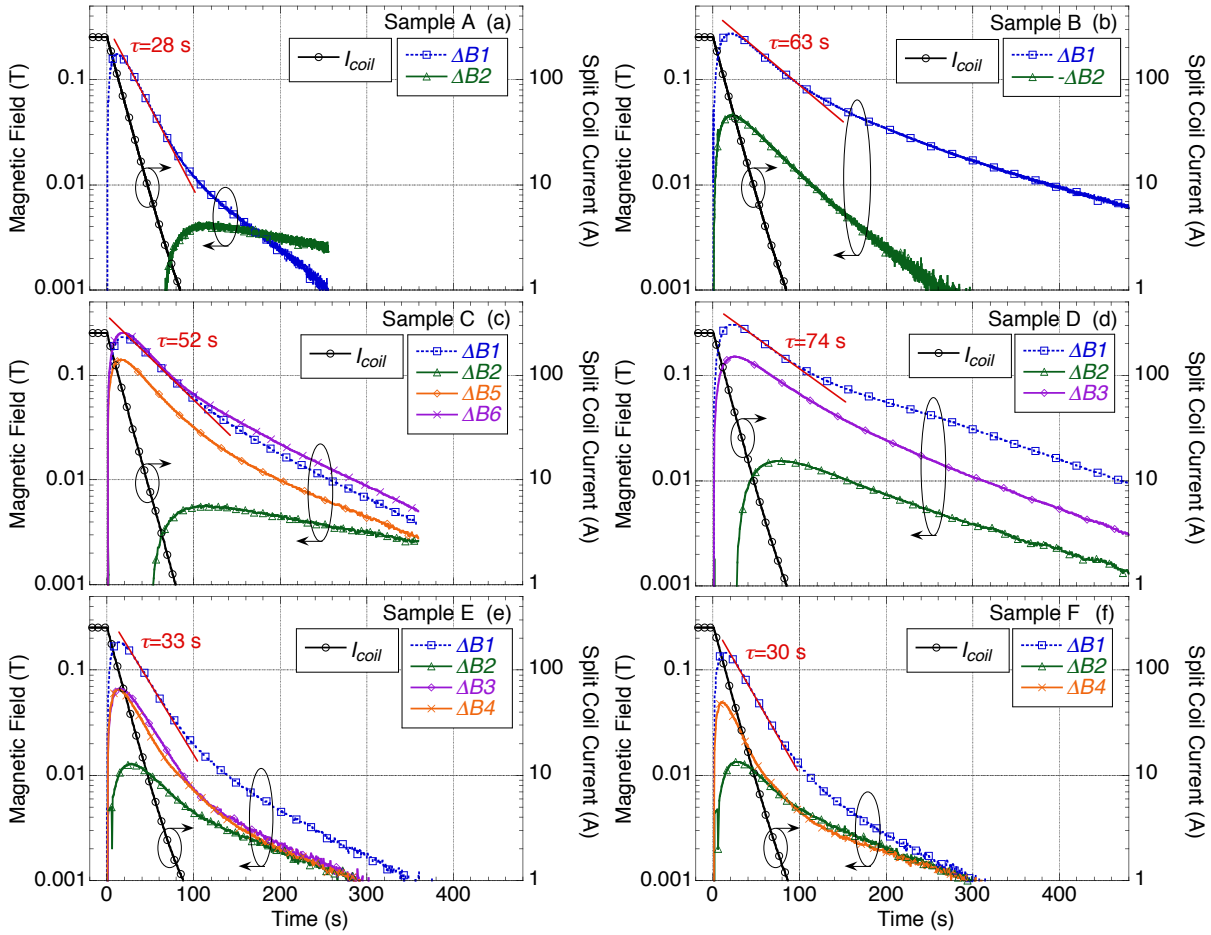


Figure 3. Estimated magnetic field by shielding currents during shut-off from -1.0 T at 4.4 K.

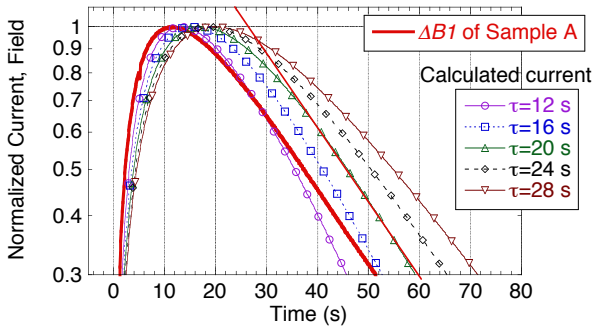


Figure 4. Calculated current of a electric circuit with a resistor R, an inductance L, and a voltage source with the decay time constant of 14.7 s for various τ=L/R. The thick line shows the magnetic field ΔB_1 of Sample A normalized by the highest value, and its decay time constant is best fitted to the calculated line with τ=20 s.

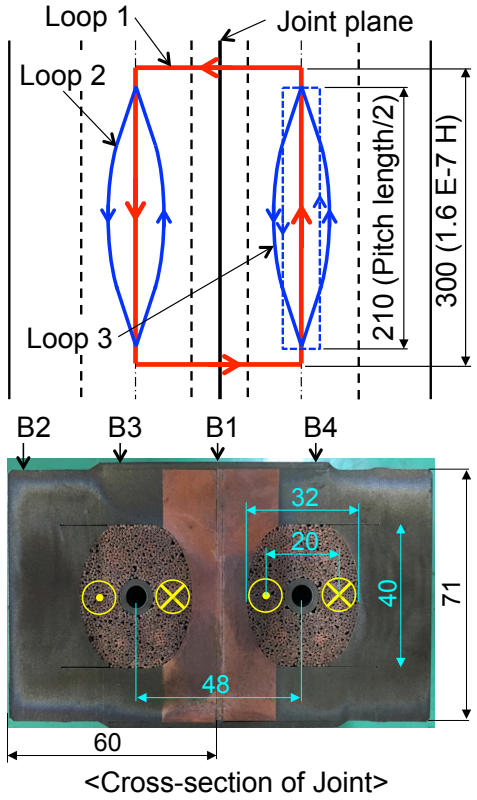
Table 1. Decay time constant and joint resistance of each sample. The decay time constants in [ ] are estimated with considering the decay time constant of the external field.

Sample	Joint resistance at 0 T, R_j (nΩ)	Decay time constant at B1, τ (s)	$4Rj\cdot\tau$ (μH)
A	2.16	28 [20]	0.24 [0.17]
B	0.61	63	0.15
C	0.79	52	0.16
D	0.52	74	0.15
E	1.48	33 [28]	0.20 [0.17]
F	1.84	30 [24]	0.22 [0.18]

4. Simulation and discussion

4.1. Simulation model

The main loop of shielding currents, Loop 1, should flow in two conductors with crossing the jointed plane twice, as shown in Fig. 5. The inductance of Loop 1 is set at 0.16 μH from the experimental data shown in Table 1. The current loops in a superconducting cable in right-leg conductor are represented by Loop 2 that is formed by the final (5th) stage sub-cables because its decay time constant should be the longest among the current loops in the cable. The inductance of Loop 2 is estimated as a set of parallel conductors with the length of 0.21 m (one-half of the twist pitch of the 5th stage), diameter of 6 mm, and distance of 20 mm. The resistance of Loop 2 is given by twice value of the average contact resistance between the superconducting strands, which is reported to be in the range of 1-30 nΩ [6-9]. The current loops in left-leg conductor are represented by Loop 3. The electric parameter of Loop 3 is assumed to be the same as Loop 2.



<Equations of electric circuits>

$$L_0\cdot dI_0/dt + M_{01}\cdot dI_1/dt + 2M_{02}\cdot dI_2/dt = -R_0\cdot I_0 \quad (2)$$

$$M_{01}\cdot dI_0/dt + L_1\cdot dI_1/dt + 2M_{12}\cdot dI_2/dt = -R_1\cdot I_1 \quad (3)$$

$$M_{02}\cdot dI_0/dt + M_{12}\cdot dI_1/dt + L_2\cdot dI_2/dt = -R_2\cdot I_2 \quad (4)$$

where L, M, R, I, and t are the self inductance, mutual inductance, resistance, current, and time. The suffixes 0, 1, and 2 mean the external field coil, Loop 1, and Loop 2, respectively. The parameters of Loop 3 are the same as Loop 2, and their mutual inductance is ignored.

<Parameters of electric circuits>

$L_0 = 2.5$ H
$R_0 = 0.17$ Ω ($\tau = 14.7$ s)
$L_1 = 0.16$ μH
$R_1 = 4R_j$
$L_2 = 0.084$ μH
$M_{01} = 56.8$ μH
$M_{02} = 10.9$ μH
$M_{12} = 0.011$ μH

Figure 5. Cross-section of joint and equivalent electric circuits for shielding currents.

4.2. Calculated results

Calculated results for Sample E are shown in Figs. 6a to 6d. In the calculation of Figs. 6a and 6b, the dependence of R_j on magnetic field is considered. From the experimental data in the case that the total current of the power supply is higher than 15 kA, the regression curve of R_j is given by

$$R_j(B) = 1.48+0.154\ B\ [\mathrm{n\Omega}] \tag{5}$$

where B [T] is the external magnetic field at the center. In the calculation of Figs. 6c and 6d, the dependence of R_j on the total current is additionally considered. According to trial and error, R_j is assumed as

$$\begin{aligned} R_j(B, I_1) &= 1.48+0.154\ B\ \ [\mathrm{n\Omega}] && \text{for } I_1 \geq 10 \text{ kA} \\ &= (1.48+0.154\ B)(1-0.67(1-I_1/10))\ \ [\mathrm{n\Omega}] && \text{for } I_1 < 10 \text{ kA} \end{aligned} \tag{6}$$

where I_1 [kA] is the current of Loop 1. R_2 is set at 5 nΩ for Figs. 6a and 6c, and 1 nΩ for Figs. 6b and 6d.

In the case of R_2 of 1 nΩ, the decay time constant of Loop 2 is longer than that of Loop 1, and the decrease of ΔB_3 is slower than ΔB_1, which differs from the experiment. Fig. 6c is in good accordance with the experiment. Therefore, the decay time constant of Loop 2 is considered to be shorter than that of Loop 1 in Sample E, and the joint resistance R_j should be decreased at low total current. This phenomenon can be simulated by the assumption of existence of few strands contacting to the copper sleeve with extremely low joint resistances [5]. The currents in the few strands should reach to the critical current at high total current, and the ratio of current flowing in the few strands becomes larger at lower total current. In this assumption, the inductance of Loop 1 is slightly changed with the total current because the current center in the cable is changed. This effect can be a cause of the phenomenon that the apparent decay time constant of Sample D around 200 s is slightly longer than that after 300 s. ΔB_1 of Sample D is considered to be increased at around 200 s with the shift of the current center.

The calculated fields in all cases are higher than the experiment, the reason of which is considered to be exclusion of current loops with shorter twist pitches in the superconducting cable as well as eddy currents in the copper sleeves.

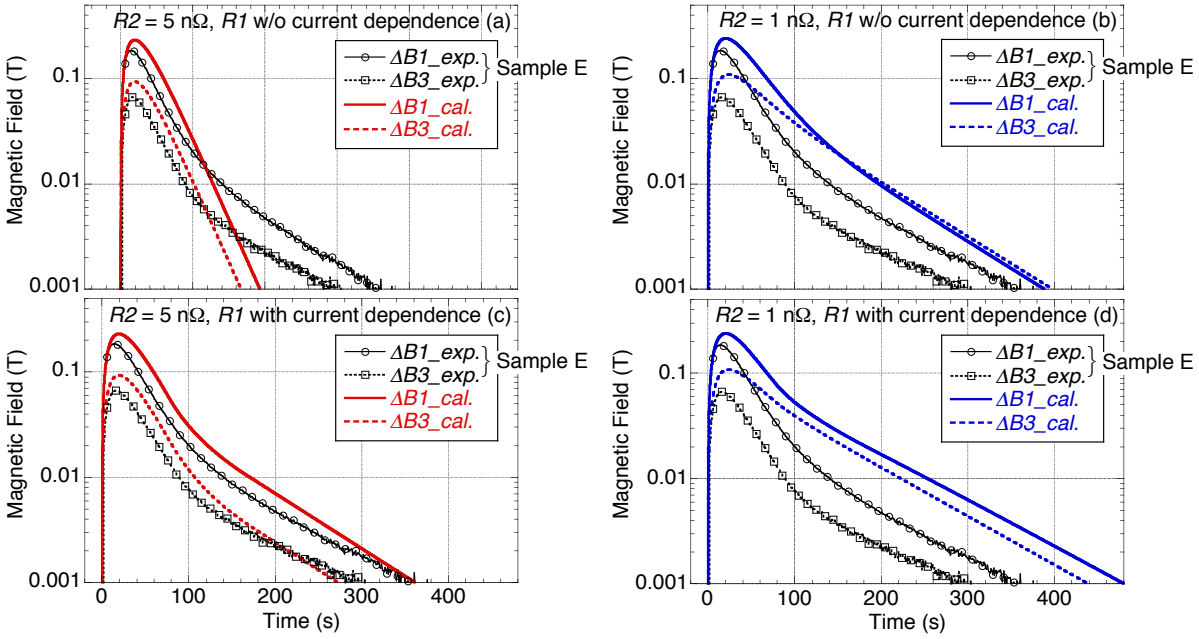


Figure 6. Calculated magnetic field by shielding currents during shut-off for Sample E. The thick lines show the calculated values, and thin lines with markers show the experimental values.

5. Summary

Shielding currents in ITER-TF joint samples were measured with Hall probes. According to evaluation of the shielding currents during shut-off of the external field coil, the main shielding current is considered to flow in superconducting cables in the two conductors with crossing the jointed plane. This decay time constant is given as $L/(4R_j)$, where L is the inductance of the current loop, and R_j is the joint resistance. The effective length of this current loop is estimated at 0.30 m, which is around three fourths of the joint length. In the case of the joint resistance around 0.5 nΩ, the main shielding current after shut-off from -1.0 T is evaluated to reach the range of 50 kA, and the highest shielding (coupling) current in each conductor is estimated to be approximately one-half of the main shielding current. Decay time constant of the main shielding current induced in the joints is gradually elongated with decrease of the current, which suggests that the joint resistance is decreased at low total current. This phenomenon can be simulated by the assumption of existence of few strands contacting to the copper sleeve with extremely low joint resistance.

*The views and opinions expressed herein do not necessarily reflect those of the ITER Organization.

Acknowledgments

This work was performed with contracted research with JAEA, collaborative research with Mitsubishi Electric Corp., collaborative research with Toshiba Corp., and the NIFS Collaboration Research program (NIFS10ULAA003, NIFS12KECA017, NIFS17KECA051).

References

[1] Sborchia C, Fu Y, Gallix R, Jong C, Knaster J and Mitchell N 2008 *IEEE Trans. Appl. Supercond.* **18** 463–66
[2] Decool P, Ciazynski D, Nobili A, Parodi S, Pesenti P, Bourquard A and Beaudet F 2001 *Fusion Eng. Des.* **58–59** 123–27
[3] Stepanov B, Bruzzone P, March S, and Sedlak K 2015 *Fusion Eng. Des.* **98-99** 1158–62
[4] Kajitani H, Hemmi T, Mizutani T, Matsui K, Yamane M, Obana T, Takada S, Hamaguchi S, Takahata K, Imagawa S and Koizumi N 2015 *IEEE Trans. Appl. Supercond.* **25** 4202204
[5] Imagawa S, Kajitani H, Obana T, Takada S, Hamaguchi S, Chikaraishi H, Takahata K, Matsui K, Hemmi T and Koizumi N 2018 *IEEE Trans. Appl. Supercond.* **28** 4200405
[6] Koizumi N, Takahashi Y, Nunoya Y, Matsui K, Ando T, Tsuji H, Okuno K, Azuma K, Fuchs A, Bruzzone P and Vecsey G 2002 *Cryogenics* **42**, 675–90
[7] Cau F and Bruzzone P 2009 *Supercond. Sci. Technol.* **22** 045012
[8] Bellina F, Breschi M and Ribani P L 2010 *IEEE Trans. Appl. Supercond.* **20** 482–86
[9] Bruzzone P, Stepanov B, Dettwiler R and Staehli F 2007 *IEEE Trans. Appl. Supercond.* **17** 1378–81